Anisotropy Effects on Chain–Chain Interactions in Stretched Rubber

J. Gao and J. H. Weiner*

Division of Engineering and Department of Physics, Brown University, Providence, Rhode Island 02912

Received July 9, 1990

ABSTRACT: When a polymer network is stretched, the distribution of chain end-to-end vectors becomes anisotropic. The effect of this anisotropy upon excluded-volume interactions between the chains of this system is studied in this paper by the molecular dynamics simulation of an idealized model of a dense system that we term an oriented melt. This is a polymer melt in which the chain vectors are maintained constant in length and direction but otherwise they and the rest of the chains are free to move. We find that in a stretched four-chain model the chain vectors cease to be a principal axis of the chain stress due to the anisotropic chain–chain interaction; this is contrary to an assumption made by us in earlier calculations on this model. We also study an oriented melt with chain vectors randomly oriented in the reference state. We find that the anisotropy in the stretched state has important effects on the chain stress and produces significant segment orientation enhancement for chains nearly perpendicular to the stretch direction. The simulations show that the stress at fixed extension increases with the reduced density $\rho = n\sigma^3/v$ where n/v is the atom number density and σ is an effective hard-sphere diameter; this is in qualitative agreement with experimental observations on the effect of large hydrostatic pressure in rubber elasticity. Finally, the simulations show clearly that on the atomic level the deviatoric or anisotropic portion of the stress in a stretched rubberlike solid is transmitted by the excluded-volume interactions, which are screened by the covalently bonded structure.

1. Introduction

An amorphous cross-linked network in the rubbery regime represents a complex system from the viewpoint of atomic interactions. Of primary interest, of course, are the covalent interactions responsible for the long-chain molecules. In addition, there are noncovalent interactions between the nonbonded atoms. The most important of the latter, and the ones we focus on here, are the strongly repulsive excluded-volume interactions. Schematically, we may represent such a system as a collection of hard spheres with covalent bonds linking them into chains that, in turn, are cross-linked at random points along their lengths.

In the classical molecular theory of rubber elasticity, these two types of interactions are regarded as affecting two independent systems: the covalently bonded chains are treated as entropic springs in tension, while the two-body spherical excluded-volume interactions are assumed to give rise only to a hydrostatic pressure as they would in a simple liquid. For the types of deformation of greatest interest, such as uniaxial extension, it is reasonable to assume that the volume of the system remains constant. Of primary interest then is the deviatoric stress, i.e., the difference between the total stress and the mean stress, and the classical molecular theory ascribes this deviatoric stress solely to the network of entropic springs.

In more recent developments of the theory, some forms of coupling between the noncovalent interactions and the covalently bonded chains are considered. These include their effect on junction fluctuations,[1,2] on their restriction of chain excursions as modeled by confining tubes,[3] and on chain entanglements.[4] Nevertheless, in these theories as well, the entropic springs retain their central role as the primary cause of the deviatoric stress.

We have been reexamining the role of the noncovalent interactions by the computer simulation of idealized atomic models of these systems.[5,6] An important characterizing parameter of dense systems with excluded volume is the reduced density $\rho = n\sigma^3/v$ where n/v is the atom number density and σ is an effective hard-sphere diameter. For rubberlike systems, as for simple fluids, it is believed that $\rho \sim 1$. Our computer simulations show that for low reduced density, $\rho \lesssim 0.4$, the noncovalent contribution to the stress is indeed almost purely hydrostatic, as assumed in the classical theory. However, for larger ρ, the noncovalent excluded-volume interactions make an increasingly significant contribution to the deviatoric stress and are dominant for $\rho \gtrsim 0.8$.

Examination of the computer simulation results in detail also makes clear the mechanism through which the spherical, two-body, excluded-volume interaction makes a nonhydrostatic contribution to the stress in a deformed rubberlike system. We find that the noncovalent interactions are screened[5] by the covalent structure, and this screening becomes more effective at higher densities. In the natural stress-free state of the system, the covalent structure is macroscopically isotropic, and therefore, the screening leaves the noncovalent contribution hydrostatic. However, when the system is deformed, the covalent structure becomes anisotropic and the screened noncovalent interactions then make a contribution to the deviatoric stress. Furthermore, as the reduced density of the system is increased, it is found that the covalent bonds are in compression[5] rather than in tension, a result that is incompatible with the simple physical picture of the chain molecule acting as an entropic spring in tension.

By application of the principles of macroscopic thermodynamics to the observed temperature dependence of the stress at constant deformation, it is readily deduced that rubber elasticity is entropic, i.e., that the restoring force is due primarily to the change in entropy upon deformation and not to the change in internal energy. It is natural, therefore, to attribute this entropy change to the change in the number of configurations available to a chain when its end-to-end distance is altered. In this connection, it is important to emphasize that a hard-sphere system interconnected by covalent bonds is also an entropic system and exhibits the proper temperature dependence of the stress at constant deformation. Therefore, the major contribution of the noncovalent interactions to

0024-9297/91/2224-1519$02.50/0 © 1991 American Chemical Society

the deviatoric stress observed in our computer simulations is fully compatible with the observed entropic character of rubber elasticity.

Chain Model. We use in this paper, as in much of our previous work, a simple chain model that has both the covalent bonding characteristic of macromolecules and the attribute of excluded volume. It approximates the hard-sphere, freely jointed chain. For computational and conceptual convenience, the covalent potential is represented by a stiff linear spring and the hard-sphere potential is replaced by the repulsive part of the Lennard-Jones potential. That is, the covalent potential $u_c(r)$ is

$$u_c(r) = {}^1/_2\kappa(r-a)^2 \tag{1}$$

where r is the distance between adjacent atoms on a given chain and a is the zero-force bond length; the noncovalent potential is

$$\begin{aligned} u_{nc}(r) &= 4\epsilon[(\sigma/r)^{12} - (\sigma/r)^6] \quad \text{for} \quad r \leq r_0 \\ &= u_{nc}(r_0) \quad \text{for} \quad r \geq r_0 \end{aligned} \tag{2}$$

where r denotes the distance between any adjacent pair of atoms on a given chain or between any pair of atoms on different chains and $r_0 = 2^{1/6}\sigma$. The results reported in this paper were all carried out, except as noted, for $\sigma = a$, $\kappa a^2/kT = 200$, and $\epsilon/kT = 0.75$. For these parameter values, the bond length undergoes only small fractional changes and σ may be regarded as an effective hard-sphere diameter.

In order to determine the stress in systems of such chains, we utilize the virial stress formula.[7] This is reviewed in section 2 where we also indicate how it may serve to introduce the concept of the chain stress, the contribution that an individual chain in an interacting system makes to its overall stress.

Limitations of Computer Modeling. Since we are relying principally on the computer simulation of idealized models of rubberlike systems for insight into the nature of stress in these materials, it is well to stress here some of the present limitations to this approach.

Real rubberlike solids are sluggish systems, with relaxation times at least on the order of minutes, for systems of macroscopic size, required to reach equilibrium after a change of conditions is imposed. Although the simulated systems are very small (on the order of 1000 atoms), it is still not possible to simulate realistic models in order to study equilibrium properties, since simulation times are limited to the order of nanoseconds even when large amounts of time on present supercomputers are available.

One of the major causes of the sluggishness in these systems is the presence of the cross-link constraints. We have devised a model system, termed an oriented melt, that provides much greater mobility and shortens relaxation times yet contains many of the significant characteristics of an amorphous cross-linked network. This model, motivated and described further in section 3, consists of a collection of interacting chains, each with a constant end-to-end vector that is free to move parallel to itself. A deformation is applied to this system through an affine transformation to its set of chain vectors while all of the other atoms of the system remain free to undergo thermal motion.

Even though the oriented melt model has far shorter time constants than a network model with fixed or fluctuating cross-links, we are still not able to simulate its behavior with all of the other governing parameters simultaneously in realistic ranges. As values of parameters such as chain length or reduced density increase, the increase in the time constant has the effect of increasing the statistical scatter between repeated simulations of reasonable computer time duration, making it difficult to draw any reliable conclusions for them. We have therefore had to limit these investigations to studying the effect of varying individual parameters or properties, while others were kept at values such that the results had reasonable reliability.

The first case we consider, in section 4, is one in which the chain vectors, in the undeformed reference state, lie in one of the four tetrahedral directions, i.e., in the directions of the four body diagonals of the unit cube. This corresponds to the model we have treated analytically in two recent papers.[8,9] There we made certain assumptions regarding the contribution to the stress made by each of the chains, and the purpose of these simulations is to test these assumptions. We find, for the chain lengths that we can simulate, that one of the assumptions made—namely, that the chain vector is a principal direction of the chain stress—is not satisfied in deformed states. This raises questions about the validity of our earlier analytical calculations as well as about some aspects of tube models.

These simulations of the four-chain model demonstrate the importance of the anisotropy of the environment on the chain stress in an interacting system of chains. In order to examine this effect further in a more realistic model, we turn next, in section 5, to the simulation of an oriented melt model in which the chain vector orientations in the undeformed reference state are uniformly distributed over the unit sphere.

A summary of the simulation results and the conclusions that can be drawn from them are contained in section 6. As we discuss in greater detail there, the atomistic character of the stress in rubberlike solids that these simulations reveal is very different from the usual view based on a picture of entropic chains in tensions. In our view, the atomistic mechanism revealed in these model studies is likely to be the operative one in real materials as well; if so, its consideration should have important consequences when considering such questions as the effect of pressure on mechanical behavior or the process of fracture initiation in elastomers.

2. Virial Stress Formula

A method for the representation of the state of stress in the network may be obtained from the generalized virial stress formula.[7] This approach, which can be derived rigorously from equilibrium statistical mechanics, treats covalent and noncovalent interactions on an equal footing and leads to the total stress tensor, deviatoric plus mean stress, in terms of time averages that can be determined from computer simulation.

For the case in which all interactions are through pair potentials, the generalized virial formula takes the form

$$vt_{ij} = -n_t kT\delta_{ij} + \sum \langle (r^\alpha)^{-1} u'_\alpha(r^\alpha) r_i^\alpha r_j^\alpha \rangle \tag{3}$$

where, in addition to previously defined quantities, v is the volume of the system, t_{ij} are the components of the stress tensor (force per unit present area) referred to a fixed rectangular cartesian system x_i, $i = 1, 2, 3$, n_t is the number of atoms free to undergo thermal motion, δ_{ij} is the Kronecker delta, α ranges over all pairs of atoms, $\mathbf{r}^\alpha$ is the vector displacement between the α pair with components r_i^α, $r^\alpha = |\mathbf{r}^\alpha|$, $u_\alpha(r^\alpha)$ is the pair potential acting between the α pair, $u'_\alpha = du_\alpha/dr^\alpha$, and brackets denote long-time averages. We may also rewrite eq 3 to make the two types

of interactions u_c and u_{nc} explicit as

$$vt_{ij} = -n_t kT\delta_{ij} + \sum_{\alpha\in c}\langle (r^\alpha)^{-1}u'_c(r^\alpha)r_i^\alpha r_j^\alpha\rangle + \sum_{\alpha\in nc}\langle (r^\alpha)^{-1}u'_{nc}(r^\alpha)r_i^\alpha r_j^\alpha\rangle \quad (4)$$

where the notations $\alpha \in c$ or $\alpha \in nc$ indicate that the sums range over all pairs of covalently or noncovalently interacting atoms, respectively.

Atom Level Stress. By dividing any pair interaction in eq 3 equally between each of the atoms in the pair, the virial formula can be written as a sum over all of the atoms of the system in the form

$$vt_{ij}/kT = \sum_\beta \langle \sigma_{ij}(\beta)\rangle \quad (5)$$

where

$$\sigma_{ij}(\beta) = -\delta_{ij} + \frac{1}{2kT}\sum_{\alpha(\beta)}(r^\alpha)^{-1}u'_\alpha(r^\alpha)r_i^\alpha r_j^\alpha \quad (6)$$

with the sum ranging over all interacting pairs to which the β atom belongs. (If β corresponds to an atom that is not free to undergo thermal motion, e.g., if it is a fixed node in a network, then the term $-\delta_{ij}$ is omitted in eq 6.) The quantity $\langle \sigma_{ij}(\beta)\rangle$ is the atomic level stress[10] associated with atom β.

Chain Stress. We next consider the contribution to the stress made by each chain of the network and we write eq 5 as

$$vt_{ij}/kT = \sum_\gamma \chi_{ij}(\gamma) \quad (7)$$

where

$$\chi_{ij}(\gamma) = \sum_{\beta(\gamma)}\langle \sigma_{ij}(\beta)\rangle \quad (8)$$

with the sum carried out over all the atoms $\beta(\gamma)$ belonging to chain γ. We call $\chi_{ij}(\gamma)$ the chain stress (referring to the laboratory frame x_i).[8]

3. Oriented Melt Model

Consider a network with fixed junctions, i.e. one in which the junctions do not undergo thermal fluctuations. Let $\mathbf{R}(\gamma)$ be the end-to-end chain vector of the γ chain in the reference network configuration and $\mathbf{r}(\gamma)$ the corresponding chain vector in the deformed configuration. It is convenient in the following discussions to regard each junction as made up of a set of fixed atoms, one for each of the chains attached to that junction. In the deformed configuration, we denote the positions of the two fixed atoms for the γ chain as $\mathbf{x}^+(\gamma)$ and $\mathbf{x}^-(\gamma)$ so that $\mathbf{r}(\gamma) = \mathbf{x}^+(\gamma) - \mathbf{x}^-(\gamma)$.

We now modify this model of a network by freeing the chain end atoms at each junction and permitting the chain end atoms also to undergo thermal motion with the proviso, however, that each chain vector remains constant, representing the same chain displacement as in the network. We refer to the resulting model as an oriented melt and impose a macroscopic deformation on it as on the corresponding network: the chain vector $\mathbf{R}(\gamma)$ in the reference configuration is transformed into the vector $\mathbf{r}(\gamma)$ in the deformed configuration by the same affine deformation that characterized the macroscopic deformation. The nature of the oriented melt model is shown schematically in Figure 1.

Our primary purpose in freeing the chains of the network to form the oriented melt is to increase atomic mobility and decrease relaxation times. However, a second purpose is served as well. In a real network, there will be many chains with the same, or essentially the same, end-to-end vector. Each of these will be in interaction with a somewhat different environment composed of chains of different lengths and orientations. We may then regard the time-averaged behavior of a particular chain of the oriented melt as representing an ensemble average of the set of chains in a large network that all have the same chain vector.

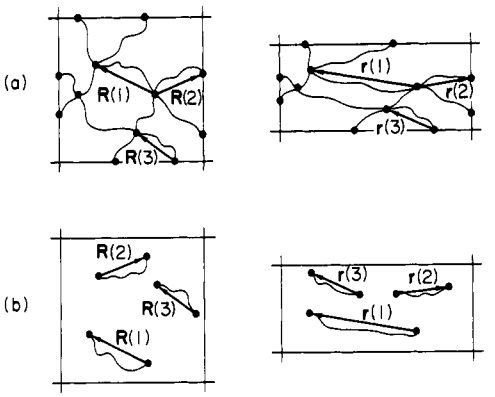

Figure 1. Oriented melt model. (a) Schematic representation of network with fixed junctions in reference state (left) and stretched state (right). Chain vectors are denoted by $\mathbf{R}(\gamma)$ in reference state and $\mathbf{r}(\gamma)$ in stretched state and are all related by same affine deformation. (b) Corresponding oriented melt. Chain vectors $\mathbf{R}(\gamma)$ and $\mathbf{r}(\gamma)$ are the same as in network and are maintained constant as to length and direction; however, they and the rest of the chain are free to move in the oriented melt.

Although there are no cross-linked junctions in the oriented melt model, its mechanical and configurational properties are closely related to those of a network with fixed junctions. Unlike the free melt, which is a liquid, the oriented melt can be deformed as a solid by imposing an affine deformation on all of chain vectors. For a system consisting of noninteracting chains, the deviatoric stress computed for the oriented melt is easily seen to be the same as that for a fixed junction network with the same chain vectors; this is also the case for the segment orientation. When interchain interaction is present, the atomic interaction near the junctions in the network may not be identical with those near the chain ends in the oriented melt; these may be important in the study of junction fluctuations and other problems related to junctions. In this paper, however, our main goal is to study the effect of interchain interaction on chain stress, on segment orientation, and on the noncovalent contribution to the macroscopic stress in a deformed network with fixed junctions. For these purposes, we assume the difference in the treatment of the junctions in the two models becomes unimportant for sufficiently long chains.

Computer Simulation. The method of molecular dynamics is used to simulate a canonical ensemble (temperature T) of an oriented melt of ν chains, each with N bonds, with periodic boundary conditions employed to remove surface effects. The basic cell has volume v so that the reduced density $\rho = n\sigma^3/v$ with $n = \nu(N+1)$. The details of the calculation procedure are similar to those employed previously for an ordinary melt.[5] The requirement that the end-to-end vectors remain constant is met by regarding the two end atoms of the chain as connected by a rigid massless rod. The forces exerted on the two end atoms then determine the motion of their center of mass; since the rod direction and length are fixed, this in turn determines the motion of the two end atoms. After an extension is imposed on the system by subjecting all of the chain vectors to the same affine deformation, the

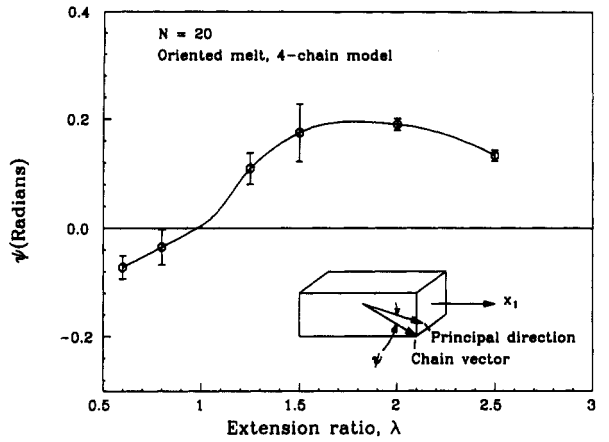

Figure 2. Angle ψ between chain vector and principal direction of chain stress for the four-chain model subjected to uniaxial extension λ. Reduced density $\rho = 0.8$.

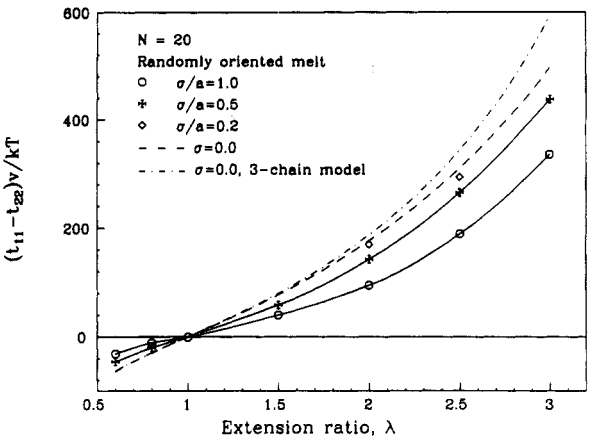

Figure 3. Stress–strain relation for randomly oriented melt subjected to uniaxial extension λ. Reduced density $\rho = 0.6$ for $\sigma/a = 1$, and $\epsilon/kT = 0.4$. Result for $\sigma = 0$ is computed analytically on the basis of eq 14. Error bars for molecular dynamics results ($\sigma > 0$) are approximately the same size as data points, $R = 4.5a$.

system stress is monitored until it reaches equilibrium; only the equilibrium values are reported here.

4. Four-Chain Model

In two recent papers,[8,9] we have treated analytically a four-chain model for rubber elasticity. The reference state corresponds to a cube with a tetrafunctional node at the center and with the chain vectors in the four tetrahedral directions; therefore, for the four-chain vectors $\mathbf{R}(\gamma)$, $|R_1(\gamma)| = |R_2(\gamma)| = |R_3(\gamma)|$.

An important assumption made in the analytical treatment of this model is that the chain vector is a principal direction of the chain stress tensor χ_{ij}. Here we consider the computer simulation of the corresponding oriented melt model performed in order to check this assumption. We treat a model with 6 chains in each of the 4 tetrahedral directions, making 24 chains per basic cell.

In the reference configuration, we do find that the chain vector is a principal direction of the chain stress tensor as is to be expected from symmetry considerations. We term this principal direction of the chain stress tensor the axial principal direction. As the model is subjected to a uniaxial extension in the x_1 direction, the simulations show that the axial principal direction ceases to be coincident with the chain vector. The resulting angle ψ between the two directions is shown in Figure 2.

This divergence between the two directions shows the importance of chain–chain interaction in the nature of the chain stress and the fact that the environment with which a particular chain interacts becomes anisotropic in the deformed system. Another way of describing the situation is that, in the deformed system, there are two axes of symmetry to consider: the chain vector and the extension direction.

Although the angle between the chain vector and the axial principal direction is not large, it does have a significant effect on the computed stress in the deformed system. The present simulation results, therefore, raise serious questions regarding the validity of the analytical calculations presented in refs 8 and 9.

5. Randomly Oriented Melt

The simulation results on the four-chain model demonstrate the importance of the anisotropy of the chain vector distribution on the nature of chain–chain interaction. We now wish to continue the examination of this question for a more realistic network model and turn next to the discussion of the simulation of an oriented melt with 48 chains in the basic cell in which the chain vector directions in the reference configuration are randomly generated corresponding to uniform probability on the unit sphere. The model is subjected to uniaxial deformation in the x_1 direction.

Stress–Strain Relation. Stress–strain curves for $N = 20$ corresponding to a fixed number density n/v and various values of σ are shown in Figure 3. It is seen that the curves show the sharp upturn in extension to be expected from the short chain length. The stress difference $t_{11} - t_{22}$ has been computed from the simulation results by means of the virial stress formulation, eq 4.

The stress–strain behavior for the same model in the absence of excluded-volume effects ($\sigma = 0$) can be computed analytically. We begin with the force–length relation $f(r)$ for a freely jointed chain with N bonds. This can be obtained from the fundamental relation[11]

$$f(r) = -kT\frac{\partial}{\partial r}\log p(r;N) \tag{9}$$

where $p(r;N)$ is the probability density for the end-to-end displacement r for the freely jointed chain; it is given by Treloar[14] as

$$p(r;N) = (8\pi ra^2)^{-1}N(N-1)\sum_{k=0}^{m}\frac{(-1)^k}{k!(N-k)!}\times \left[\frac{N-(r/a)-2k}{2}\right]^{N-2} \tag{10}$$

with m being the integer in the interval

$$[N-(r/a)]/2 - 1 \le m < [N-(r/a)]/2 \tag{11}$$

The stress t_{ij} is then obtained from $f(r)$ by the relation[13]

$$t_{ij} = \frac{1}{v}\sum_{\gamma}\frac{f(r(\gamma))r_i(\gamma)r_j(\gamma)}{r(\gamma)} - p\delta_{ij} \tag{12}$$

where the hydrostatic pressure p is arbitrary. For the stress difference $t_{11} - t_{22}$, eq 12 becomes

$$t_{11} - t_{22} = t_{11} - {}^1/_2(t_{22} + t_{33}) = \frac{1}{v}\sum_{\gamma} f(r(\gamma))r(\gamma)(\cos^2\phi(\gamma) - {}^1/_2\sin^2\phi(\gamma)) \tag{13}$$

where $\phi(\gamma)$ is the angle that the γ chain makes with the x_1 axis in the deformed state. For a large number of chains, the sum in eq 13 can be rewritten as an integral that can

be put in the following form:

$$t_{11} - t_{22} = \frac{\nu}{4\upsilon}\int_{-1}^{+1} f(r(\alpha,\lambda))\, r(\alpha,\lambda)\left(\frac{3\lambda^3\alpha^2}{(\lambda^3-1)\alpha^2+1} - 1\right) d\alpha \tag{14}$$

where

$$r(\alpha,\lambda) = R[(\lambda^2 - \lambda^{-1})\alpha^2 + \lambda^{-1}]^{1/2} \tag{15}$$

with $\alpha = \cos\phi_0$, where ϕ_0 is the angle between the chain and the x_1 axis in the reference state, R is the chain length in the reference state, and ν is the number of chains in volume υ. Note that the uniform distribution of chain vector orientation over the sphere in the reference state implies uniform distribution with respect to α. For a specified $f(r)$ relation, it is straightforward to evaluate numerically the integral in eq 14 for arbitrary values of λ. For $f(r)$ linear, corresponding to a Gaussian chain, eq 14 reduced to the familiar classical molecular result. The result of the use of eq 14 for the randomly distributed chain vectors of the oriented melt is also shown in Figure 3. It is compared there with the results of the molecular dynamics calculations for σ = 1.0, 0.5, and 0.2, with all other parameters held fixed. It is seen that the molecular dynamics results for small σ approach the analytical values for $\sigma = 0$. This serves as a check on the accuracy of our molecular dynamics program for interacting chains. It is also of interest to note that the equilibrium stress in this model system with excluded volume is less than that in the corresponding ideal system and decreases with increasing σ.

Three-Chain Model. A frequently used approach for the analysis of non-Gaussian effects, due to short chains, is to employ the familiar three-chain model,[14,15] in which it is assumed that the chain orientations in the reference state lie equally in the three coordinate directions, x_1, x_2, and x_3. As noted by Treloar,[14] the three-chain model is strictly valid only for Gaussian chains; i.e., it gives the same result as the distribution of chain vectors uniform over the sphere when Gaussian chains are employed. This equality, however, is a consequence of the linear character of the force law for Gaussian chains, and it is of interest to compare, in Figure 3, the result of the three-chain model with that for the more accurate formulation of eq 14. It is seen that the three-chain model relation is in good agreement with the uniform distribution result only for small λ where the force law is linear but becomes increasingly inaccurate for large λ, precisely where non-Gaussian effects are of interest.

Entropic Character. As a check on the entropic character of the elasticity of the model, the internal energy of the system is computed for each value of λ as the time average of the total energy; it is found to be independent of λ to within <0.2%.

Chain Stress. The computer simulation program also determines the chain stress $\chi_{ij}(\gamma)$ for each of the individual chains in the randomly oriented melt by use of eqs 6 and 8. In order to determine the effect of the anisotropy of the chain vector distribution in the deformed system on the chain–chain interaction and therefore on $\chi_{ij}(\gamma)$, we compare these quantities with those obtained from the simulation of the corresponding free melt, i.e., one obtained from the oriented melt by removing the constraint that the chain vectors remain constant. In the free melt simulation, the value of the chain stress is computed for each chain at each time step and is referred to as a local coordinate system $\bar{x}_m$ with one axis $\bar{x}_1$ in the chain vector direction. This leads to the instantaneous value of what we have termed[8] the intrinsic, $\bar{\chi}_{mn}(\mathbf{r}(\gamma))$, where our notation makes explicit the instantaneous value $\mathbf{r}(\gamma)$ of the chain vector. The program sorts and averages over time and all chains the values of $\bar{\chi}_{mn}(\mathbf{r}(\gamma))$ according to $|\mathbf{r}(\gamma)|$, leading to the tensor functions $\bar{\chi}_{mn}(r)$. It is clear from the method of computation that $\bar{\chi}_{mn}(r)$ should be a cylindrical tensor with $\bar{\chi}_{11}$, $\bar{\chi}_{22} = \bar{\chi}_{33}$, the only non-zero components, and this is found to be the case within small numerical scatter.

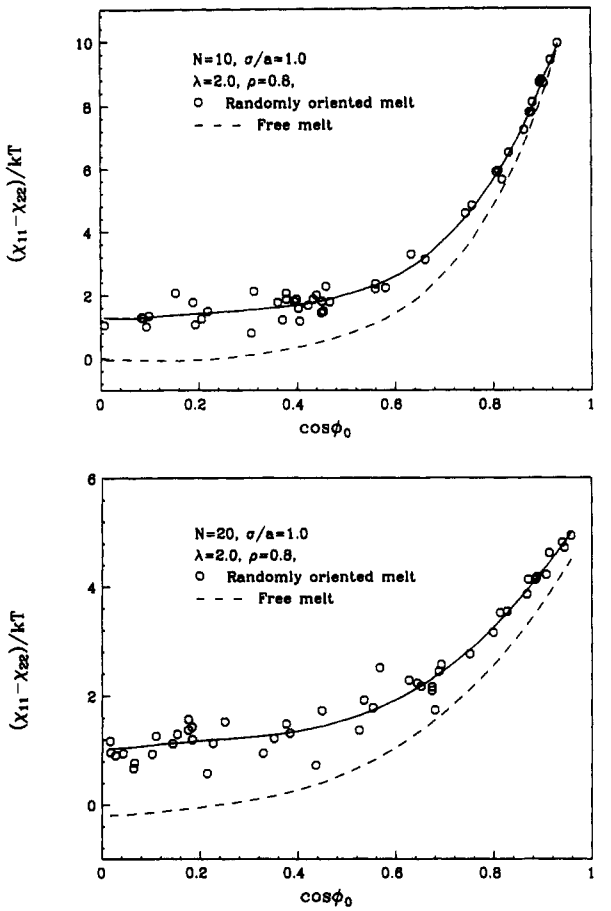

Figure 4. Chain stress difference $\chi_{11} - \chi_{22}$ (eq 8) as determined by molecular dynamics simulations for randomly oriented melt and for corresponding ordinary free melt. Angle ϕ_0 is measured between chain vector and stretch axis x_1 in the reference state. (a) Chain has N = 10 bonds, $R = 3.5a$. (b) N = 20, $R = 4.5a$.

We can now determine $\chi^*_{ij}(\gamma)$, the chain stress of chain γ in the oriented melt as if it had interacted with an isotropic environment, by means of the tensor transform

$$\chi^*_{ij}(\gamma) = \bar{\chi}_{mn} a_{mi}(\gamma) a_{ni}(\gamma) \tag{16}$$

where $a_{mi}(\gamma)$ are the direction cosines between $\bar{x}_m(\gamma)$, the intrinsic coordinate system for chain γ in the oriented melt, and x_i, the laboratory frame.

A comparison between $\chi^*_{ij}(\gamma)$ and the actual chain stress in the oriented melt, $\chi_{ij}(\gamma)$, is shown in Figure 4 for the case of uniaxial extension where only the differences $\chi_{11} - \chi_{22}$ are of interest. It is seen that the effect of the anisotropic environment is substantial and that the values of $\chi^*_{11} - \chi^*_{22}$ are consistently below those of $\chi_{11} - \chi_{22}$, with the difference being greatest for chains perpendicular to the stretch direction. Note that simulation results for quantities such as $\chi_{11} - \chi_{22}$ that refer to a single chain show larger numerical scatter than for quantities such as $t_{11} - t_{22}$ that involve data collected for the entire system.

Segment Orientation. We may gain some insight into the mechanism whereby the anisotropic environment enhances the chain stress by examination of the segment

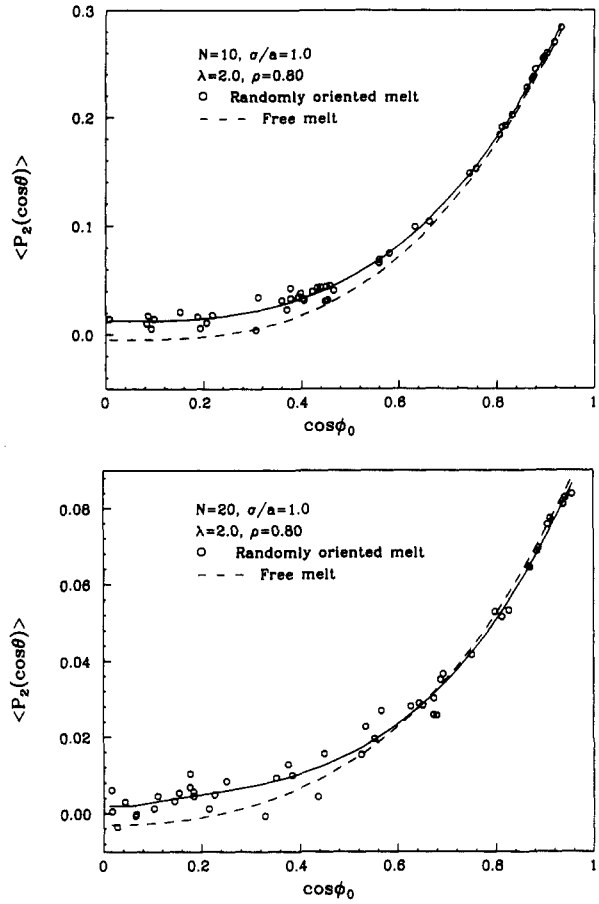

Figure 5. Segment orientation $\langle P_2(\cos\theta)\rangle$ (eq 17) where θ is the angle between segment and stretch axis x_1. Each data point represents average over time and over all segments for given chain identified by angle ϕ_0 with stretch axis in reference state. (a) $N = 10$, $R = 3.5a$ (b) $N = 20$, $R = 4.5a$.

orientation $\langle P_2(\cos\theta)\rangle$ where

$$P_2(\cos\theta) = {}^1/_2(3\cos^2\theta - 1) \qquad (17)$$

and where θ is the angle between the segment and the stretch direction in the oriented melt. For comparison purposes, we also compute $P_2(\cos\bar{\theta})$ for the segment orientation in the free melt, with $\bar{\theta}$ measured from the chain vector, and use this function to determine the value of $\langle P^*_2(\cos\theta)\rangle$ for the different chains in the oriented melt to be expected if they had interacted with an isotropic environment. The comparison is shown in Figure 5. It is seen that the anisotropic chain vector distribution causes an enhancement of segment orientation that is most pronounced for chains perpendicular to the stretch direction, and it is this which is responsible, in part, for the increase in stress for these chains. The enhancement of segment orientation seen in these model calculations is in accord with proposals put forward as explanations of NMR observations on strained networks.[17,18]

Noncovalent Contribution to Stress. By the use of eq 4, it is possible to determine separately the contributions of the covalent and noncovalent potentials to the stress difference $t_{11} - t_{22}$ in the stretched oriented melt model. The result is shown in Figure 6. It is seen that as the reduced density ρ increases the covalent contribution becomes negative (i.e., compressive) while the noncovalent contribution increases steadily and becomes dominant for $\rho \gtrsim 0.8$. This is in accord with earlier simulations of network models with fixed cross-links; those calculations, however, involved much larger numerical scatter, and the oriented melt model yields much more clear-cut results.

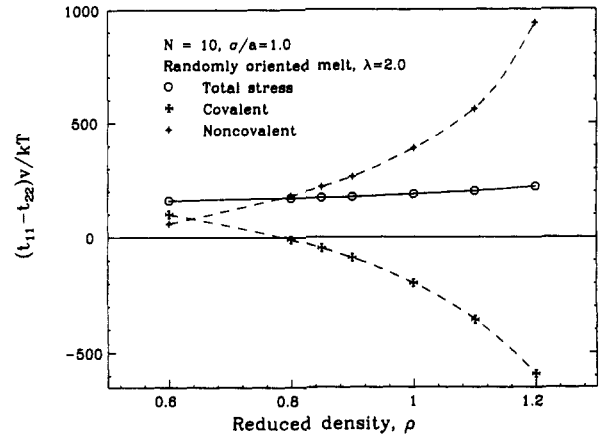

Figure 6. Covalent and noncovalent contributions to the stress $t_{11} - t_{22}$ in randomly oriented melt subjected to uniaxial extension $\lambda = 2$. The variation in the reduced density ρ is produced by variation in system volume v, while σ is held fixed. Increase in total stress with increase in ρ is also shown.

It is also clear from the present simulations, as shown in Figure 6, that the total stress $t_{11} - t_{22}$ (that is, the sum of covalent and noncovalent contributions) shows, at fixed extension, an increase with ρ; the observed increase, it should be noted, is greater than that to be expected, on the basis of the molecular theory, due solely to the decrease in volume of the system. This result is in qualitative accord with the experiments of Questad et al.,[24] who find a large increase in $t_{11} - t_{22}$ for a polyurethane elastomer (Solethane 113) in the rubberlike regime under large increase of imposed hydrostatic pressure. They also find a large increase in the strain to fracture with increasing pressure. If fracture initiation by covalent bond scission is postulated, then the fact that the covalent bonds are observed to be increasing in compression as the reduced density is increased in the computer simulations may provide an explanation for the experimental results.

6. Summary and Conclusions

The equilibrium properties of a polymer melt, time-averaged over a sufficiently long period, are inherently isotropic. Its isotropic character is exhibited not only by all of its global properties but also by each of its component chains. Thus, the overall state of stress is purely hydrostatic in an equilibrium polymer melt, and each of its chains makes only a hydrostatic contribution to the stress.

When a melt is cross-linked into a network, isotropy is first lost at the chain level. In the melt, the end-to-end vector $\mathbf{r}$ of an arbitrary chain must have zero time average, $\langle\mathbf{r}\rangle = 0$, due to its tumbling motion; in the network, on the other hand, we have $\langle\mathbf{r}\rangle \neq 0$ due to the cross-link constraints. Therefore, the stress contribution of an individual chain will, in general, be anisotropic. However, for a network with an isotropic distribution of chain vectors, the global or macroscopic stress distribution will remain isotropic. It is only after the network is deformed that the chain vector distribution and the corresponding macroscopic stress distribution become anisotropic.

In this paper, we have studied, by the computer simulation of idealized models, the effect of the anisotropic distribution of chain vectors in a deformed network upon the nature of chain–chain interaction. The following conclusions can be drawn:

(a) This anisotropy has a significant effect upon the chain stress $\chi_{ij}(\gamma)$, the contribution to the overall stress in the network made by chain γ, eqs 8 and 6.

(b) We find, in particular, for the four-chain model previously studied by us[8,9] that as a result of the anisotropy the end-to-end vector of chain γ is not a principal direction of $\chi_{ij}(\gamma)$. This contradicts an assumption made in our analytical treatment of this model, and this approach toward a molecular explanation of the Mooney effect must be reexamined.

(c) The oriented melt model introduced in this paper appears to be a valuable approach to the study of these questions. It incorporates the ability to control the chain vectors and their distribution as in a cross-linked network, while its relaxation time constants are substantially shorter. As a result, molecular dynamics simulations with reasonable computer times lead to results with much smaller numerical scatter than the models with fixed cross-links.

(d) The simulations show clearly that interchain excluded-volume interactions in the deformed anisotropic system result in enhanced segment orientation, particularly for chains originally perpendicular to the stretch direction. These observations are in accord with earlier simulations performed by us[16] on the three-chain model of rubber elasticity. Enhanced segment orientation has been observed in experiments utilizing NMR[17,18] and fluorescence polarization[19] in strained networks. Theoretical treatments of these phenomena include the work of Tanaka and Allen[20] extending the analysis of DiMarzio,[21] and more recent treatments[22,23] that model enhanced segment orientation by introducing a phenomonological orientational-dependent term in the expression for the free energy per segment. Our simulations demonstrate that the enhanced segment orientation effect occurs naturally in the system, even with excluded volume modeled by a spherically symmetric repulsive potential.

(e) The simulation of an oriented melt with chain vector orientations uniformly distributed over the unit sphere in the reference state shows clearly the increasingly significant noncovalent excluded-volume contribution to the deviatoric stress in the deformed state. For reduced density $\rho \gtrsim 0.8$, these contributions are dominant, Figure 6. These results confirm, with much less numerical scatter, previous simulations of other types of models.

(f) The simulations show that the stress difference $t_{11} - t_{22}$ for constant uniaxial extension in the x_1 direction increases with increasing density ρ. This result is in qualitative accord with the observed stress increase at constant extension under large imposed hydrostatic pressure.[24]

(g) A byproduct of our calculations on the randomly oriented melt is a demonstration that the use of the familiar three-chain model for the calculation of non-Gaussian effects in uniaxial extension involves substantial errors at large values of the extension ratio λ, precisely where non-Gaussian effects are of interest.

Although the oriented melt model has much smaller time constants than a model with fixed cross-links, it has still not been possible to simulate systems with long chains at high system density. Therefore, the present work has been limited to systems of chains with $N = 10$ and 20 bonds. Further model and algorithm development will be necessary to study the behavior of longer chains. On the basis of other simulations involving longer chains in free melts in which we have computed what we have termed intrinsic atomic level stresses,[10] however, we believe that the large noncovalent contribution to the stresses in dense systems described in this paper will be found to apply to network models with more realistic chain lengths as well. This description of the atomic nature of stress in rubberlike systems is very different from the usual molecular level description involving entropic springs in tension. While the molecular level picture may be more convenient for computation, it appears to us that the atomic level description is closer to physical reality. In particular, it may have physical consequences, such as the effect of pressure[24] upon the deviatoric stress or upon the strain to fracture, that are difficult to explain in terms of a molecular theory.

Acknowledgment. This work has been supported by the Gas Research Institute (Contract 5085-260-1152). The computations were performed on the Cray Y-MP at the Pittsburgh Supercomputing Center.

References and Notes

(1) Ronca, G.; Allegra, G. *J. Chem. Phys.* **1975**, *63*, 4990.
(2) Flory, P. J.; Erman, B. *Macromolecules* **1982**, *15*, 900.
(3) Gaylord, R. J.; Douglas, J. F. *Polym. Bull.* **1987**, *18*, 347.
(4) Doi, M.; Edwards, S. F. *J. Chem. Soc., Faraday Trans. 2* **1978**, *74*, 1802.
(5) Gao, J.; Weiner, J. H. *Macromolecules* **1989**, *22*, 979.
(6) Weiner, J. H.; Gao, J. In *Molecular Basis of Polymer Networks*; Baumgartner, A., Picot, C. E., Eds.; Springer-Verlag: Berlin, 1989.
(7) Gao, J.; Weiner, J. H. *Macromolecules* **1987**, *20*, 2520.
(8) Weiner, J. H.; Gao, J. *Macromolecules* **1989**, *22*, 4544.
(9) Weiner, J. H.; Gao, J. *Macromolecules* **1990**, *23*, 1860.
(10) Gao, J.; Weiner, J. H. *J. Chem. Phys.* **1989**, *90*, 6749.
(11) See, for example: Weiner, J. H. *Statistical Mechanics of Elasticity*; Wiley, New York, 1983; p 234.
(12) Flory, P. J. *Statistical Mechanics of Chain Molecules*; Interscience: New York, 1969; p 315.
(13) See, for example: Doi, M.; Edwards, S. F. *The Theory of Polymer Dynamics*; Clarendon: Oxford, 1986; p 74.
(14) Treloar, L. R. G. *The Physics of Rubber Elasticity*, 3rd ed.; Clarendon: Oxford, 1975; p 113 et seq.
(15) Debolt, L. C.; Mark, J. E. *J. Polym. Sci., Part B: Polym. Phys.* **1988**, *26*, 865.
(16) Gao, J.; Weiner, J. H. *Macromolecules* **1988**, *21*, 773.
(17) Deloche, B.; Samulski, E. T. *Macromolecules* **1981**, *14*, 575.
(18) Sotta, P.; Deloche, B. *Macromolecules* **1990**, *23*, 1999.
(19) Queslel, J.-P.; Monnerie, L.; Erman, B. *J. Macromol. Sci.—Chem.* **1989**, *A26*, 93.
(20) Tanaka, T.; Allen, G. *Macromolecules* **1977**, *10*, 426.
(21) DiMarzio, E. *J. Chem. Phys.* **1962**, *36*, 1563.
(22) Jarry, J.; Monnerie, L. *Macromolecules* **1979**, *12*, 316.
(23) Deloche, B.; Samulski, E. T. *Macromolecules* **1988**, *21*, 3107.
(24) See Figures 2 and 3 in: Questad, D. L.; Pae, K. D.; Scheinbeim, J. I.; Newman, B. A. *J. Appl. Phys.* **1981**, *52*, 5977.